

Resonances in transfer-triggered breakup of ${}^7\text{Li}$ in near-barrier collisions

E. C. Simpson^{1,a}, K. J. Cook¹, M. Dasgupta¹, S. Kalkal¹, D. H. Luong¹, I. P. Carter¹, D. J. Hinde¹, and E. Williams¹

¹Department of Nuclear Physics, Research School of Physics and Engineering, The Australian National University, Canberra, ACT 2601, Australia

Abstract. Above-barrier complete fusion cross sections of weakly-bound ${}^6,7\text{Li}$ and ${}^9\text{Be}$ are known to be suppressed with respect to single-barrier penetration model calculations. Breakup of the projectile — either via direct excitation of continuum states, or by transfer of nucleons — is thought to be the cause, preventing complete capture of the projectile charge. Using the example of ${}^7\text{Li} \rightarrow {}^8\text{Be} \rightarrow \alpha + \alpha$ we show how the contributions to breakup from different resonances in ${}^8\text{Be}$ can be identified, and discuss their likely influence on fusion.

1 Breakup and fusion suppression

Above-barrier fusion of light, weakly-bound projectiles such as ${}^7\text{Li}$ is known to be suppressed [1–3]: single-barrier penetration model calculations, which accurately model fusion of strongly-bound projectiles such as ${}^{18}\text{O}$, overestimate measured fusion cross sections for weakly bound ${}^7\text{Li}$ by $\sim 25\%$ (see Ref. [4] for a recent review). Breakup reactions are thought to reduce the probability for fusion of the entire projectile. Both direct breakup (${}^7\text{Li} \rightarrow \alpha + t$) and transfer-induced breakup (e.g., ${}^7\text{Li} \xrightarrow{+p} {}^8\text{Be} \rightarrow \alpha + \alpha$, ${}^7\text{Li} \xrightarrow{-n} {}^6\text{Li} \rightarrow \alpha + d$, ${}^7\text{Li} \xrightarrow{-2n} {}^5\text{Li} \rightarrow \alpha + p$) have been found to be important with ${}^{208}\text{Pb}$ and ${}^{209}\text{Bi}$ targets [5, 6].

Understanding the detail of these breakup processes is crucial to understand their influence on fusion. Breakup can only suppress complete fusion when the disintegration occurs when the projectile and target nucleus are approaching one another. However, from below-barrier measurements of breakup, where incomplete fusion is negligible, it is known that breakup often proceeds via long-lived resonance states [2]. These states, such as the ${}^8\text{Be}$ ground state, survive until the ejectile is very far from the target, and *cannot* suppress fusion. Short-lived states will decay much nearer the target, but even sub-zeptosecond ($< 10^{-21}$ s) lifetimes may be sufficient to alter whether the projectile-like nucleus breaks up prior to reaching the fusion barrier, and therefore reduce the impact of breakup on fusion.

To investigate these effects we consider the example of proton pickup by ${}^7\text{Li}$ on a ${}^{58}\text{Ni}$ target, giving ${}^8\text{Be}$. ${}^8\text{Be}$ is unbound with respect to decay into $\alpha + \alpha$, with the narrow 0^+ ground state 0.092 MeV above the threshold, and a broad 2^+ resonance at 3.12 MeV [7]. The ${}^{58}\text{Ni}$ target is chosen to reduce, with respect to heavier ${}^{208}\text{Pb}$ -region targets, the influence that the target has on the trajectories of the fragments following breakup. Identification of asymptotic

and near-target breakup, classical dynamical simulations of the resultant α fragment trajectories, and their respective influence on fusion is discussed below.

2 Identifying asymptotic breakup

When investigating the impact of breakup on fusion, the most important characteristic of the reaction is where (and when) the breakup occurs. Only if the projectile breaks up prior to reaching the fusion barrier will it affect fusion. At above barrier energies, it is likely that one or other of the fragments may still fuse with the target, giving a contribution to incomplete fusion, and making it harder to study the breakup itself. A series of measurements at below barrier energies has been made at the Australian National University Heavy Ion Accelerator Facility to clarify the detail of the breakup mechanism. The measurements used the BALiN double-sided silicon-strip detector array [8] to detect the energies E_i and angles (θ_i, ϕ_i) of the resulting pairs of charged fragments detected in coincidence.

The relative energy of the fragments $E_{rel} = \frac{1}{2}\mu v_{12}^2$ gives a basic way to distinguish between breakup of long-lived states and that occurring near the target nucleus. Long-lived states have a well defined energy that is unperturbed by any differential acceleration of the fragments by the (highly remote) target following breakup. As such, when the relative energy of the fragments is reconstructed, these states appear as narrow peaks in the E_{rel} spectrum. The example of ${}^7\text{Li} \xrightarrow{+p} {}^8\text{Be} \rightarrow \alpha-\alpha$ is shown in Fig. 1, for a ${}^{58}\text{Ni}$ target with a beam energy of 13.1 MeV ($\sim 0.95V_B$). The data is gated on the 2.981-MeV $1/2^+$ state in ${}^{57}\text{Co}$, which is strongly populated in other proton pickup reactions with ${}^7\text{Li}$ [9]. The red shaded region highlights the narrow peak associated with the ${}^8\text{Be}$ ground state, which sits on an exponentially decaying background.

^ae-mail: edward.simpson@anu.edu.au

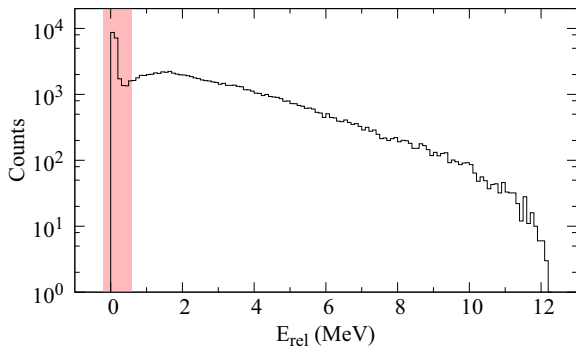


Figure 1. The relative energy of the two fragments can be used to separate near-target and asymptotic breakup. Shown are the measured α - α relative energies for ${}^7\text{Li}+{}^{58}\text{Ni}$ collisions. Long-lived states, such as the ${}^8\text{Be}$ ground state highlighted by the red area, decay very far from the target, and as such, the relative energy of the α s remains equal to the energy of the state. The exponentially decaying component of the distribution is assumed to result from breakup near the target.

3 Near-target breakup

Whilst asymptotic breakup manifests as a narrow peak in the relative energy distribution, the origin of the remainder — the featureless, exponential background — is less clear. It has previously been assumed [5, 6] that it arises from breakup near the target nucleus. Half of these events were assumed to occur as the reaction partners approached one another, therefore half were supposed capable of suppressing fusion. For the case of ${}^9\text{Be}\rightarrow{}^8\text{Be}\rightarrow\alpha+\alpha$, it was suggested that the near-target breakup might proceed via instantaneous breakup of the ${}^8\text{Be}$ 2^+ state [10]. Were it not for the presence of the target, the 2^+ would give a peak at $E_{rel} = 3.12$ MeV.

A more refined understanding is desirable. Useful insights can be obtained by studying the distribution of events as a function of the fragment opening angle θ_{12} , and the orientation of the fragments' relative motion with respect to that of their centre of mass, β [11, 12]. The opening angle θ_{12} is typically strongly correlated with the relative energy E_{rel} (see e.g., Fig. 8(a) of Ref. [6]). If the relative motion is aligned with the motion of their centre-of-mass in the laboratory ($\beta = 0^\circ$ and $\beta = 180^\circ$), then the opening angle θ_{12} will be minimised. Conversely, if the relative motion is perpendicular to that of the centre-of-mass ($\beta = 90^\circ$), the θ_{12} will be maximised and, for the case of fragments of identical mass, the energies of the fragments E_1 and E_2 will be equal. If there is no acceleration of the α fragments by the target following breakup, there is a well defined relationship between the orientation angle β and the opening angle of the two fragments θ_{12} for a given relative energy E_{rel} (the asymptotic correlation).

Differential acceleration of the fragments following breakup distorts this relationship. The experimental data are shown in Fig. 2 compared to the expectations for asymptotic breakup of the ${}^8\text{Be}$ 0^+ ($E_{rel} = 0.092$ MeV) and 2^+ ($E_{rel} = 3.12$ MeV) states. Since the two fragments are

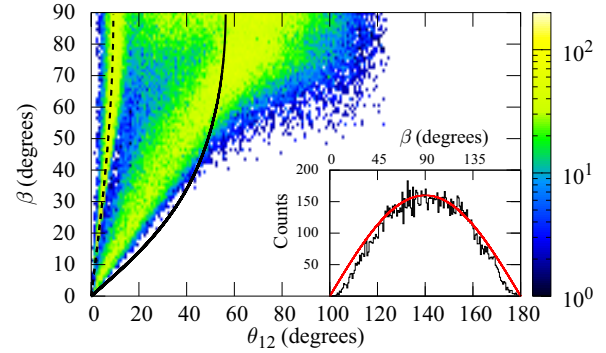


Figure 2. The distribution of data with respect to the angles θ_{12} and β , shown here for ${}^7\text{Li}+{}^{58}\text{Ni}$. The dashed and solid lines indicate the expected correlation for asymptotic decay of the ${}^8\text{Be}$ 0^+ and 2^+ states respectively. The 0^+ band is clearly asymptotic, whereas the 2^+ is not. The inset shows the projection of the ground state band onto β , which is consistent with isotropic emission ($\sin\beta$ curve shown in red).

identical, the data is symmetric about $\beta = 90^\circ$ and has been folded about this point. The data is limited to $\theta_{12} < 132^\circ$ — with limited efficiency for the largest θ_{12} — due to the incomplete coverage of the BALIN detector array.

Two bands are seen in the data. The band on the left is associated with breakup via the ${}^8\text{Be}$ 0^+ ground state, and clearly follows the expected asymptotic correlation (dashed line). Projected onto β (inset of Fig. 2), the sinusoidal distribution for this band indicates isotropic breakup. The second band does not follow the asymptotic expectation, but it is interesting that it arises from the almost featureless relative energy distribution. The relative closeness to the asymptotic prediction for the ${}^8\text{Be}$ 2^+ (solid line) suggests these events do indeed originate from this state.

4 Modelling post-breakup acceleration

To investigate how the distribution of events with β and θ_{12} is sensitive to the location of breakup, we need to model the trajectories of the fragments after breakup. Assuming that near-target breakup originates from ${}^8\text{Be}$ in the 2^+ resonant state, the initial relative energy of the fragments will be equal to the resonance energy, $E_R = 3.12$ MeV [7]. How the α particles accelerate will depend on (a) their orientation with respect to the target [13], and (b) their distance from the target. This is illustrated in Fig. 3.

To investigate this further we make Monte Carlo simulations using a modified version of the PLATYPUS code [14, 15] to model post-breakup acceleration effects. The breakup location is fixed at some point Δr on the projectile-target trajectory, where here Δr is some radial distance after the distance of closest approach R_0 . This is illustrated in Fig. 4. The fragments are initially placed with their centre of mass at the breakup location, and are separated by a distance equal to their mutual barrier radius (~ 6 fm). Breakup is thus defined to occur when the two fragments have passed their mutual barrier. Prior to this

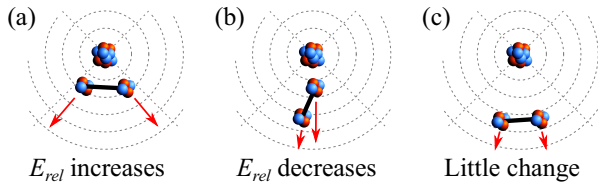


Figure 3. The acceleration of the fragments, following breakup, depends on their initial orientation with respect to the target nucleus. (a) If the relative vector of the α -particles is aligned perpendicular to the field of the target, the post-breakup acceleration will increase the α - α relative energy. (b) Conversely, alignment with the field will tend to reduce the relative energy. (c) The magnitude of the acceleration depends on the proximity to the target - the further from the target, the smaller the post-breakup acceleration.

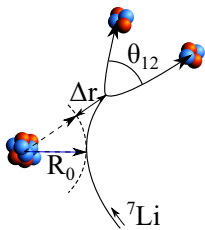


Figure 4. Illustration of the projectile-target trajectory. In the simulations, breakup is assumed to occur at some fixed radial distance Δr after the distance of closest approach R_0 has been passed. The opening angle of the fragment asymptotic velocity vectors is θ_{12} .

point, we assume that the fragments remain sufficiently well localised so as not to affect fusion. Tidal forces generated by the target may be important in hastening or indeed hindering breakup, but this is beyond the scope of the present discussion. The orientation of the α - α relative position vector is randomly sampled from an isotropic distribution. Having set these initial conditions, the fragments and target propagate according to their mutual Coulomb interactions, and the simulation is continued until all three are sufficiently far apart. Five hundred events are sampled to construct the correlation between asymptotic quantities β and θ_{12} . Further details can be found in Ref. [12].

5 Results for ${}^7\text{Li} \rightarrow {}^8\text{Be} \rightarrow \alpha + \alpha$

Here we focus on events when the projectile-like and target-like nuclei are receding from each other. Breakup prior to the projectile reaching the distance of closest approach, and the effects of resonance width and projectile-target angular momentum, are discussed in Ref. [12]. The present calculations are for zero projectile-target angular momentum, and this axial symmetry means that for each calculation all events lie along a single line. The results for distances $\Delta r = 1, 2, 4, 10$ and 1000 fm after the distance of closest approach are shown in Fig. 5. At 1000 fm the breakup is essentially asymptotic, and the correlation found agrees with the analytic expectation shown in Fig. 2. As the breakup point moves inwards towards the target nucleus, the correlation becomes distorted. For those events where the α s are aligned with the target potential [e.g., Fig. 3(b)], the acceleration reduces the relative energy and θ_{12} . For the α particles aligned perpendicular to the potential, the acceleration increases the relative energy and θ_{12} .

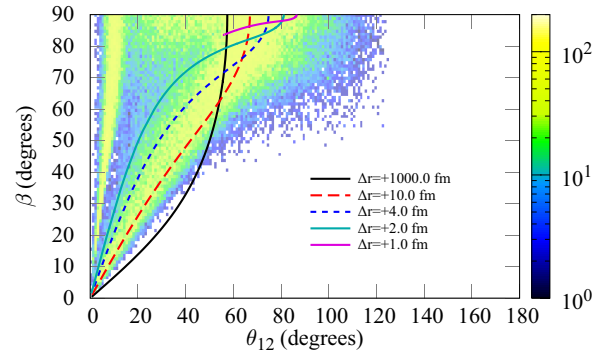


Figure 5. Data and simulations showing the correlation between β and θ_{12} . See the text for further discussion.

As the distance becomes smaller the distortions become stronger. For the smallest distance, $\Delta r = 1$ fm, nearly all the energy is locked into the fragment-target potential. The release of this energy, in essentially independent interactions of the fragments with the target, gives fragments with very similar energies. As a result, all 500 events reconstruct to β values near 90° .

The results of the simulations suggest that much of what is seen in the present experiment arises from breakup occurring only once the projectile and target have receded by several femtometers from the distance of closest approach. Breakup when the two are approaching tends to lead to large θ_{12} which the current experiment is not sensitive to — further details can be found in Ref. [12].

6 Consequences for fusion

These results suggest that the properties of short-lived resonances [16, 17], such as the ${}^8\text{Be} 2^+$, may play an important role in determining the extent to which breakup suppresses fusion. This is illustrated in Fig. 6. The plot shows the radial separation of the projectile and target as a function of time for a sample trajectory, coloured by the anticipated transfer probability. This transfer probability is expected to fall exponentially with increasing separation (see e.g., [14, 18]). The transfer probability is peaked at the distance of closest approach, but if the state populated by the transfer has a lifetime of 0.5 zs, the breakup locations will be shifted (approximately) along the trajectory to later times (shown in green). This lifetime effect could explain why the simulations suggest breakup occurs primarily when the projectile and target are already moving apart. Moreover, at above barrier energies the reactants will have crossed the fusion barrier before the resonant state has had a chance to disintegrate, and so fusion will not be suppressed.

7 Conclusions and outlook

The correlation between β and θ_{12} appears to be sensitive to the distance between the projectile-like and target-like nuclei at the point of breakup. The properties of broad

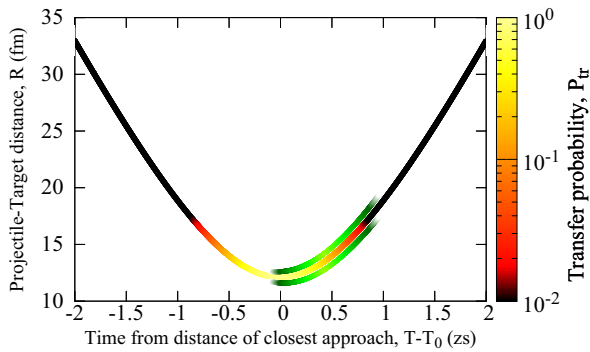


Figure 6. Illustration of the influence of short-lived states on breakup. The yellow-red-black line shows the projectile-target trajectory as a function of the time from the distance of closest approach and projectile-target separation R . It is coloured by the transfer probability, which peaks at the distance of closest approach and falls exponentially, as show in the inset. The green region indicates the approximate breakup location, shifted due to the unbound state populated having a short lifetime (~ 0.5 zs).

resonant states may be very important in determining this distance, and therefore the consequences for fusion. To further understand the influence of breakup on fusion, new measurements are required on a variety of targets to focus on large opening angles θ_{12} , to study breakup occurring prior to the distance of closest approach. More sophisticated classical dynamical modelling must also be performed, taking into account both narrow and broad resonances and their characteristic shapes and lifetimes.

Furthermore, every nucleus, particularly every light nucleus, is different. Due to differences in their structure the results found for β vs. θ_{12} for ${}^6\text{Li} \rightarrow \alpha + d$ and ${}^7\text{Li} \rightarrow \alpha + t$ coincidences are very different from those shown here — both have long-lived narrow states, and though they show evidence of near-target breakup, neither has low-lying broad resonant states similar to the ${}^8\text{Be}^{2+}$. The consequences for fusion may therefore be rather different, and require further detailed investigations.

Acknowledgements

Helpful discussions with A. Diaz-Torres are gratefully acknowledged. We thank M. Evers, L. R. Gasques, P. R. S. Gomes,

R. Linares and A. Wakhle for their assistance in running the experiment. Support from Australian Research Council grants FL110100098, DP130101569, DE140100784 and DP14101337 is acknowledged. Support for accelerator operations through the NCRIS program is acknowledged.

References

- [1] M. Dasgupta, D. J. Hinde, K. Hagino *et al.*, *Phys. Rev. C* **66**, 041602(R) (2002).
- [2] D. J. Hinde, M. Dasgupta, B. R. Fulton *et al.*, *Phys. Rev. Lett.* **89**, 272701 (2002).
- [3] M. Dasgupta, P. R. S. Gomes, D. J. Hinde *et al.*, *Phys. Rev. C* **70**, 024606 (2004).
- [4] L. F. Canto, P. R. S. Gomes, R. Donangelo *et al.*, *Phys. Rep.* **596**, 105 (2015).
- [5] D. H. Luong, M. Dasgupta, D. J. Hinde *et al.*, *Phys. Lett. B* **695**, 105 (2011).
- [6] D. H. Luong, M. Dasgupta, D. J. Hinde *et al.*, *Phys. Rev. C* **88**, 034609 (2013).
- [7] D. R. Tilley, J. H. Kelley, J. L. Godwin *et al.*, *Nucl. Phys. A* **745**, 155 (2004).
- [8] D. H. Luong, K. J. Cook, E. Williams *et al.*, *Proc. of Sci. Pos(NIC XII)*, 185 (2012).
- [9] A. Marinov, W. Oelert, S. Gopal *et al.*, *Nucl. Phys. A* **438**, 429 (1985).
- [10] R. Rafiei, R. du Rietz, D. H. Luong *et al.*, *Phys. Rev. C* **81**, 024601 (2010).
- [11] A. B. McIntosh, S. Hudan, C. J. Metelko *et al.*, *Phys. Rev. Lett.* **99**, 132701 (2007).
- [12] E. C. Simpson, K. J. Cook, D. H. Luong *et al.*, *Phys. Rev. C* **93**, 024605 (2016).
- [13] J. E. Mason, S. B. Gazes, R. B. Roberts *et al.*, *Phys. Rev. C* **45**, 2870 (1992).
- [14] A. Diaz-Torres, D. J. Hinde, J. A. Tostevin *et al.*, *Phys. Rev. Lett.* **98**, 152701 (2007).
- [15] A. Diaz-Torres, *Comp. Phys. Comm.* **182**, 1100 (2011).
- [16] A. M. Lane and R. G. Thomas, *Rev. Mod. Phys.* **30**, 257 (1958).
- [17] F. C. Barker, *Aust. Jour. Phys.* **41**, 743 (1988).
- [18] S. Saha, Y. K. Agarwal and C. V. K. Baba, *Phys. Rev. C* **49**, 2578 (1994).